**National Science Foundation**

**Research Experience for Undergraduates**

# Interface Issues in Chemical Vapor Deposited Aluminum Oxide on Silicon

**Patrick Mahoney**

**Qiana Carswell**

**Department of Chemical Engineering**

**University of Illinois at Chicago**

**Advanced Materials Research Laboratory**

August 1, 2002

**Table of Contents:**

**Abstract:**

Alumina ($Al_2O_3$) has emerged as one of the promising substitutes for the $SiO_2$ dielectric layer currently used in semiconductor devices. It is necessary to replace Silicon Dioxde if further performance gains are to made in these devices. Alumina has risen to become a promising candidate due to its high dielectric constant, offset conduction band energy to Si, and its strength to withstand high-temperature processing. Experimental studies[1] have shown, however, that postdeposition annealing of the films at 900°C gives rise a $SiO_2$ layer at the film-substrate interface. Our aim was to study the process conditions of $SiO_2$ formation, interfacial chemistry and interface theory of the system.

# I. Introduction

## 1.1 History of MOSFET

Complementary Metal Oxide Semiconductor (CMOS) chips consist of arrays of Metal Oxide Semiconductor Field Effect Transistors (MOSFET). The MOSFET is one type of transistor and is the fundamental unit in a CMOS chip. CMOS chips have continually seen increases in performance. However, the electronics industry continues to expect and demand still greater performance. It is the job of researchers to find new ways of meeting these demands.

Performance increases are obtained through "scaling", shrinking the dimensions of the MOSFET. A key element in the ability to scale a MOSFET is the dielectric layer and its properties.

## 1.2 Manufacturing

A MOSFET is a device that is built onto a silicon substrate in CMOS chips. Simply, a MOSFET is a switch whose state (on or off) can be controlled via an applied voltage at the "gate". Several types of MOSFETs exist; all are similar, and only one will be described here. The gate forms a capacitor with the silicon substrate. Application of a voltage at the gate creates a conducting channel in the silicon substrate through which current can flow between the source and the drain ("on" state). Removal of the voltage destroys the conducting channel, and the MOSFET is in the "off" state.

### 1.2.1 Dielectric Layer

The dielectric layer sits between the gate and the silicon substrate. The dielectric allows the electric field at the gate to penetrate into the substrate thereby creating the

conducting channel. The dielectric must also prevent current flow between the gate and the substrate.

Currently, silicon dioxide is used as the dielectric layer in CMOS chips. Silicon dioxide is the natural choice due to its long history of use, its stability atop silicon, and the ease with which it is formed on silicon.

**1.3 Current Limitations**

As MOSFETs are scaled down, the capacitance at the gate must be increased. The capacitance obeys the following equation[2]:

$$C = \kappa\varepsilon_0 A/t \qquad (1)$$

where C = capacitance

$\kappa$ = dielectric constant (of the dielectric layer)

$\varepsilon_0$ = permittivity of free space

A = area of the capacitor

t = thickness of the dielectric

To increase capacitance, one must increase either $\kappa$ or A, or decrease t. "A" cannot be increased; MOSFETs are being scaled *down*. A change in $\kappa$ would require a change in dielectric material. The remaining option, "t", is the parameter that is currently being changed as MOSFETs are scaled.

Unfortunately, a limit exists on the thickness of silicon dioxide that will soon be reached. The physical size of the $SiO_2$ bonds require at least 7Å of thickness; studies have shown a practical limit for $SiO_2$ at ~13Å[2].

### 1.4 Aluminum Oxide as a Replacement

As the thickness limit for $SiO_2$ is approached, use of new materials with higher dielectric constants ($\kappa$) in replacement of $SiO_2$ becomes necessary in order to meet capacitance demands while allowing attainable thicknesses. One possiblity for replacing $SiO_2$ is aluminum oxide. Aluminum oxide has several key advantages that make it a very promising candidate. First, of course, it has a higher $\kappa$ value than $SiO_2$ (9 vs. 3.9)[2]. Stoichiometric $Al_2O_3$ is thermodynamically stable on silicon. Finally, it has a sufficiently high energy of conduction compared to that of silicon. Were this value too low, current could leak to the gate from the conducting band in the silicon substrate[2].

#### 1.4.1 Methods of Deposition

In our experiment, aluminum oxide is deposited onto silicon using a technique called Metal Organic Chemical Vapor Deposition (MOCVD). An organic precursor containing a metal (Trimethyl aluminum) is first deposited onto the substrate in the form of a chemical vapor. It is next reacted with the appropriate chemical (oxygen) to yield the desired product (aluminum oxide).

As stated before, stoichiometric $Al_2O_3$ is thermodynamically stable on silicon. MOCVD of aluminum oxide does not necessarily yield stoichiometric $Al_2O_3$. Our reactor may actually yield $Al_2O_{3+x}$. Previous research has shown that upon annealing at 500ºC of samples prepared by MOCVD of aluminum oxide, an interfacial layer of silicon dioxide forms between the silicon and aluminum oxide. It has been hypothesized that the extra oxygen in $Al_2O_{3+x}$ fuels the interfacial SiO2. This is significant because the annealing at 500ºC simulates conditions experienced during the manufacture of CMOS chips. Many steps are involved in the manufacture of CMOS chips, some of which

require high temperatures. It is important that aluminum oxide be able to withstand these typical CMOS processing conditions. The silicon dioxide that forms is undesirable as it becomes a part of the dielectric layer and effectively limits the dielectric properties of aluminum oxide. It will be necessary to have the ability to control the interfacial silicon dioxde before the aluminum oxide can be used in CMOS chips.

### 1.5 Purpose for this summer

The purpose of our research was to study this interfacial layer of silicon dioxide. In particular, we wished to study the effects of deposition conditions and annealing conditions on the formation of the interfacial layer of silicon dioxide.

## II: Experimental Procedure

### 2.1 Standard Cleaning Procedure

The wafers were diced into 15 mm×22 mm samples using a diamond cutter. The substrate was rinsed in dionized water for 7 minutes and then dried in nitrogen gas. We soaked the sample in 1:2 parts H2SO4:H2O2 solution for 1 hour to remove organic contaminates. After this we soaked the substrate in HF solution for 30-60 seconds, rinsed it, and dried in nitrogen. We measured thickness of native SiO2 using ellipsometry. The suggested native oxide thickness should be no greater than 4-6 Angstroms for deposition and no more than 0 Angstroms for microscopy.

### 2.2 Deposition

The MOCVD system used in the experiments was a custom made reactor. The reaction chamber contained a sample holder, two input gas lines, and one exhaust line attached to a vacuum pump. The sample was heated with a quartz halogen lamp while a

PID controller (Eurotherm Inc., Virginia) was used to maintain the substrate temperature at ±2ºC of the desired set point (300ºC). Pressure during operation was maintained at 0.5 Torr. The bubbler contained the aluminum precursor, trimethyl aluminum (TMA). Argon was bubbled at 30 ±5 sccm to deliver the precursor into the chamber. The line between the bubbler and the chamber was heated to 40ºC to prevent condensation of the TMA in the gas line. A purge argon flow was maintained in a separate line that merged with the bubbler line before entering the reactor. A separate line delivered oxygen into the chamber at variable flow rate (10 and 30 sccm). (See Figure 1)

The deposition of each sample consisted of a similar procedure. After loading the sample and ramping the temperature to the 300ºC, the deposition was performed in cycles. One cycle consisted of flowing Ar through the bubbler for 30s followed by 30s of oxygen. The purge argon remained open throughout the deposition. A typical deposition consisted of 20 cycles of this type. Upon completion, the thickness of the deposited film (aluminum oxide) was measured with ellipsometry.

### 2.2.1 MOCVD System Characterization

We performed an experiment to characterize the deposition rate of our reactor. We used six single polished CZ wafers. Depositions were performed on two wafers each at three different temperatures (100 ºC, 200º C, 300 ºC). Measurements of the Alumina growth were taken with ellipsometry at various points throughout the depositions. The results are plotted in Figure 2. In Figure 3, the results show the average growth rate per cycle. It can be seen that as temperature increases the average growth rate decreases. This is due to the fact that the TMA is adsorbed on to the substrate; as temperature

increases adsorption rate decreases. The average growth rate is between 3-7 Angstroms per cycle, this approaches atomic layer control[2]. This is important because atomic layer control give a sharp interface and regulation of the final film thickness.

### 2.3 Ellipsometry

The Ellipsometer we used to measure thickness in this experiment was the WVASE 32 (See Figure 4). After initialization of the hardware we placed the sample on the stage, began set up, and acquired the scan. The Ellipsometer is capable of analyzing multilayer structures like $Al_2O_3/SiO_2/Si$. Since ellipsometry is an optical technique that requires an accurate model of the measurement process to analyze data, it is helpful to first characterize the single films in order to find their optical constants. The thickness of the single films should be similar to the thickness of the corresponding film in case the material exhibits thickness dependent optical constants. The Ellipsometer gives us optical constants which in turn can give us several values, namely thickness.

#### 2.3.1 Optical Constants

Optical constants are parameters which characterize how a material will respond to excitation by an Electro Magnetic fields at a given frequency. Within WVASE32 the optical constants are expressed as[2]:

Complex Dielectric Function represents the degree to which the material may be polarized by an applied electric field.

$$\acute{\varepsilon}=\varepsilon_1+\iota\varepsilon_2 \qquad (2)$$

Complex refractive index represents the effect the material has on an Electromagnetic wave propagating through the material.

$$\acute{\eta}=\eta+\iota k \qquad (3)$$

The functions are related by the equation:

$$\acute{\varepsilon}=\acute{\eta}^2 \qquad (4)$$

Visually, the sample is exposed to polarized light and the Ellipsometer measures the polarization state of the reflected beam. This method of thickness measurement is non-destructive, and there is zero sample preparation.

### 2.4 FT-IR Analysis

The main analysis of our samples was performed using Fourier Transform Infrared Spectroscopy (FT-IR) (See Figure 5). Different vibrational modes in chemical bonds absorb different, characteristic frequencies of radiation. The FT-IR machine takes advantage of this fact. A sample to be analyzed is exposed to a range of IR radiation (wavenumbers of 400 to 1400 $cm^{-1}$). A detector determines which frequencies have been absorbed by the sample and therefore which bonds are present in the sample. The process is nondestructive and requires no sample preparation.

#### 2.4.1 Sample FT-IR Spectrum

In our work, we were concerned with the detection of $SiO_2$. The spectral peak for $SiO_2$ occurs at wavenumbers between 1050 and 1060 $cm^{-1}$. Figure 6 shows spectra obtained at five minute intervals during annealing of one of our samples. Not only can FT-IR be used to determine the presence of bonds, but it can also be used to determine the quantity of a bond. Our spectra demonstrate this and show the amount of $SiO_2$ increasing as annealing progresses.

#### 2.4.2 Phonon Frequency Shift

Phonon frequency shift is a phenomenon that occurs in FT-IR Spectra. In Figure 7 one can see the Transverse Optical (TO) Phonon and Longitudinal Optical (LO)

Phonons. The TO Phonon which appears at a wavenumber of 1050, is associated with asymmetric stretch of Oxygen in the $SiO_2$ bond. The LO Phonon appearing at 1250, demonstrates how light interacts with a change in angle. In Figure 7, one can observe that frequency will vary with film thickness due to change in the structural and chemical nature of the film.

### 2.4.3 Annealing

After deposition of aluminum oxide the samples are annealed in the furnace at a temperature of 500°C. There is a constant flow of Argon through the furnace to provide an inert environment. Annealing is done in an attempt to simulate temperature conditions similar to those of semiconductor fabrication. Figure 8 is a diagram of the result of the deposition and annealing process. In essence if we cannot eliminate the SiO2 layer formation, then the process needs to be optimized to minimize and control the SiO2 layer.

## 2.5 JEOL JEM2010F Analysis

We deposited Alumina on two samples for Scanning Transmission Electron Microscopy Analysis. Neither sample had been annealed. The samples had the same oxygen flow rate during deposition (10 standard cubic centimeters) as well as deposition chamber temperature (200ºC). However, the thicknesses were different. STEM 020625-1 had a thickness of 160 Angstroms. STEM 020702-1 had a thickness of 220 Angstroms.

### 2.5.1 Preparation for STEM

The best type of build to study the interface is the cross-sectional sample (See Figure 10). It is composed of two slices of the sample bonded with M-610 Bond. Next we ground the sample to 20 μm on a lapping table with diamond lapping film. We used a film thickness vs. color chart to recognize a 20μm thickness was obtained. Next we

attached the sample to a 3mm copper ring with M-610 Bond. The ring, with sample, was then placed inside the ion mill that bombarded the sample with Argon ions until the sample was electron transparent. The angles of incidence were 12º, 10º, 8º for 30, 60, and 20 min respectively at a voltage of 3kV.

The result was a fully prepared sample for the STEM (See Figure 11a). There is a hole through the center and the edges are thinner than the rest of the sample. Figure 11b is a picture of our first sample. One can see that it is not milled directly in the center, but off to one side; this is because it was ground slightly unevenly. Therefore, the Ar ions milled through the thinner side more easily. The STEM probe will be aimed at the hole. Part will go straight through the middle and the rest will hit the sides and transmit information to the detector below.

### 2.5.2 Electron Energy Loss Spectroscopy (EELS)

One of the special techniques that can be done with the JEOL JEM2010F is Electron Energy loss Spectroscopy (EELS). The reason we do EELS is so that we can separate inelastically scattered electrons and qualify the information they contain[5]. The physical properties that we are investigating using EELS are a possible phase change and the acquisition of optical constants. We hypothesize that a possible phase change may occur above a certain temperature. It is possible that when annealed we no longer have the desired amorphous (α-) alumina, but possibly gamma (γ-), crystalline, alumina. EELS uses VUV spectroscopy and can plot the interband transition strength versus various transitions from ionic and covalent bonding. Optical constants can be acquired with EELS much the same way as through ellipsometry.

## III. Results & Discussion

### 3.1 $O_2$ Flow rate experiment

We performed experiments to study the effects of oxygen flow rate during deposition on $SiO_2$ formation during annealing. Five samples (double polished CZ Si (100) wafers) were first cleaned using our standard cleaning procedure described previously. Alumina was deposited on the samples in our MOCVD chamber. Three samples were deposited with 30 sccm of oxygen, and the remaining two were deposited at 10 sccm. All other deposition conditions were the same including temperature (300 ºC), pressure (0.5 Torr), and flow rate of Argon through the TMA bubbler (30 sccm).

Annealings were performed at 500ºC in an Argon environment. FT-IR spectra were taken at 5 min intervals during each anneal. The samples were removed from the furnace, taken to the FT-IR machine, and later replaced into the furnace for continued annealing. *Figure 12* shows the peak heights of the $SiO_2$ peaks as measured by FT-IR for each sample. The peak heights have arbitrary units. In order to convert the heights to actual thicknesses, we used work done previously by Abhijit Chowduhri (AMReL, UIC). He compared ellipsometric data to FT-IR spectra and obtained a linear relation between the thickness reported by ellipsometry and the FT-IR peak heights. We applied this to our data and obtained *Figure 13* which shows $SiO_2$ thickness vs. annealing time. Finally, we normalized the $SiO_2$ thickness data to the initial $Al_2O_3$ thickness and graphed the $SiO_2$ thickness ratio vs. annealing time in *Figure 14.* This was done to account for the fact that each sample had a different thickness of $Al_2O_3$.

### 3.2 STEM Images

We obtain Z-Contrast STEM images for sample STEM 020625-1 (See Figures 15, 16, 17). The Annular Dark Field images show the Alumiumn Oxide deposited on the Silicon substrate. The images are original, unprocessed and unfiltered. We measured a Aluminum oxide thickness of 160 Angstroms using ellipsometry. Using the rough scale provided on the image the thickness appears to be 190 Angstroms. However, this measurement is not the exact thickness measured by the STEM.

## IV. Conclusions

### 4.1 $O_2$ Flow rate experiment

The graphs show the initial growth of $SiO_2$ followed by a trailing off as the $SiO_2$ reaches an equilibrium thickness. At first glance the data do not appear to show any conclusive results. However, if one considers samples B and Z to be outliers, the data become more interesting. The furnace did not allow fine temperature control. Samples B and Z were annealed together, and it is possible the temperature was not at 500 ºC. The remaining three samples, two at 30 sccm and one at 10 sccm of oxygen, all have equilibrium ratios between 0.1 and 0.2. This agrees with data previously obtained by A. Chowduhri. It is not unreasonable that the data from samples B and Z are indeed outliers. If this is the case, we can conclude that oxygen flow rate during deposition has no significant effect on $SiO_2$ formation. Unfortunately, time constraints prevent us from performing further experiments in this area.

### 4.2 STEM Images

In Figure 17, we begin to see a third layer forming between the Aluminum oxide and the Silicon substrate. Coarse analysis reveled that this layer is less than 10

Angstroms and contains Aluminum and Oxygen. More analysis, including EELS spectra, needs to be completed to study whether Silicon is also present.

### 4.3 Future Experiments

Future experiments include gathering complete EELS Spectra And Analysis on the interfacial SiO2 and Aluminum oxide layer of an unannealed and annealed sample.

## V. Acknowledgements

We would like to thank the National Science Foundation Research Experience for Undergraduates Program for funding. We would also like to thank the Department of Chemical Engineering, the Advance Materials Research Laboratory, and the Department of Physics @ University of Illinois at Chicago. Specifically we would like to thank Abhijit Chowdhuri, Sayeeram Pillur Mahadevan, Yuanyuan Lei and Prof. Christos Takoudis for their priceless assistance.

**References**


2. A. Roy Chowdhuri and C. G. Takoudis, Appl. Phys Lett. 4241, 80 (2002).
3. G.D. Wilk, Appl. Phys. Rev. 5223, 89 (2001).
4. Adsorption of Molecules on Surfaces
5. http://www.chem.qmw.ac.uk/surfaces/scc/scat2.htm
6. Guide to Using WVASE 32, J.A. Woollam Co., Lincoln NE, 1999.
7. David B. Williams, C. Barry Carter, Transmission Electron Microscopy. Plenum Press, New York.
8. http://www.fairchildsemi.com/an/AN/AN-9010.pdf

# Figures

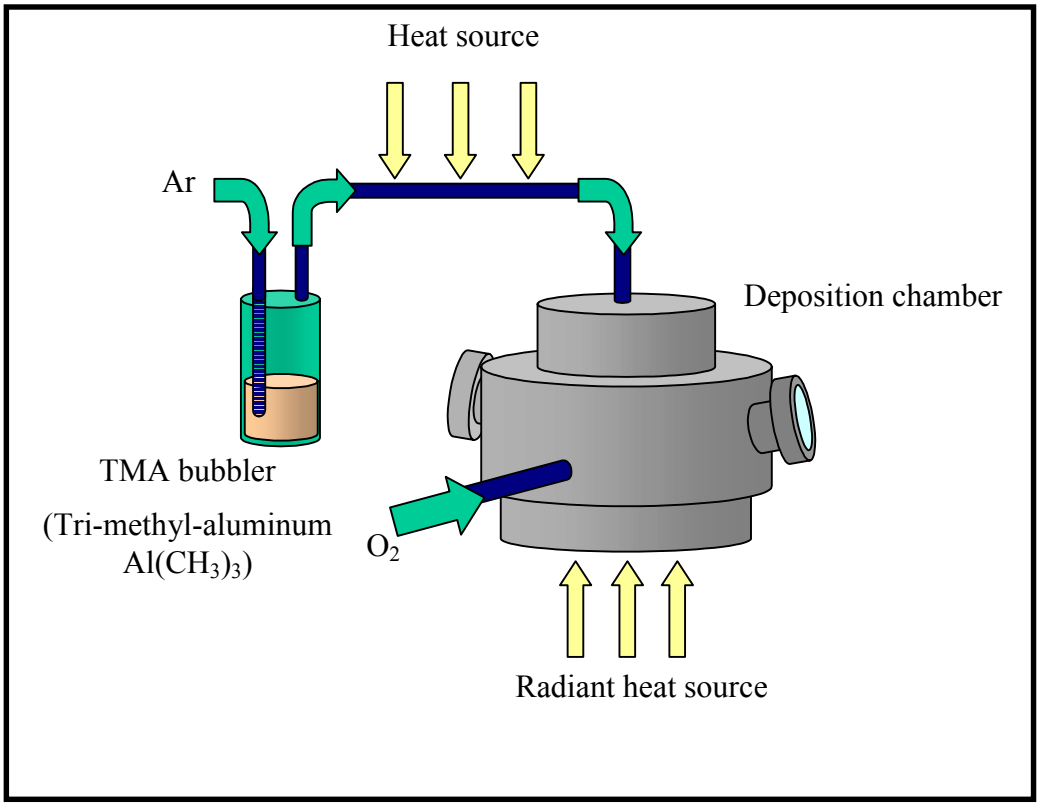


Figure 1: Schematic of MOCVD system

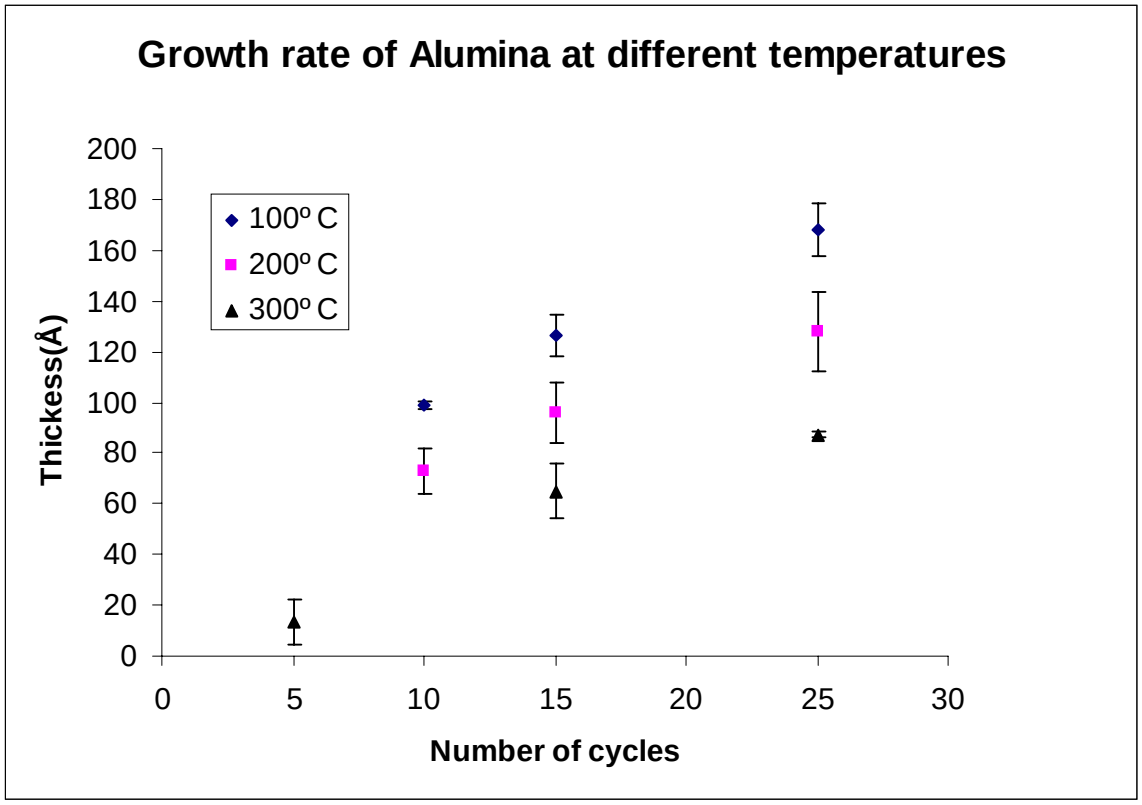


Figure 2: Growth of alumina at different temperatures in custom reactor

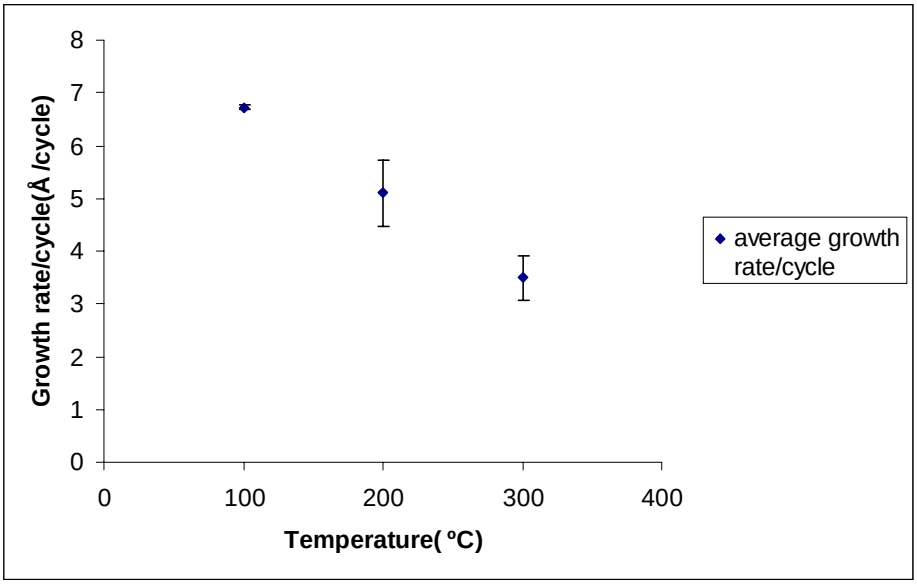


Figure 3: Growth rate of alumina in custom reactor

Figure 4: Ellipsometer

Figure 5: FTIR bench

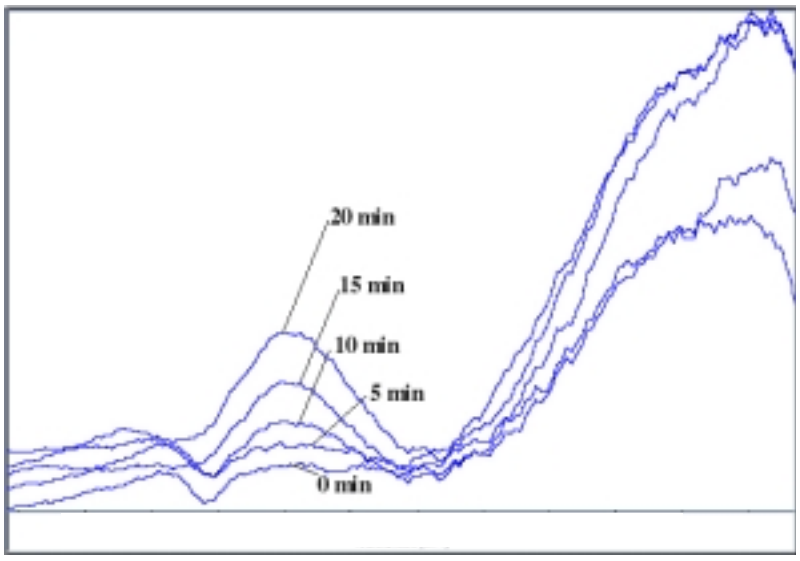


Figure 6: Sample FT-IR Spectra

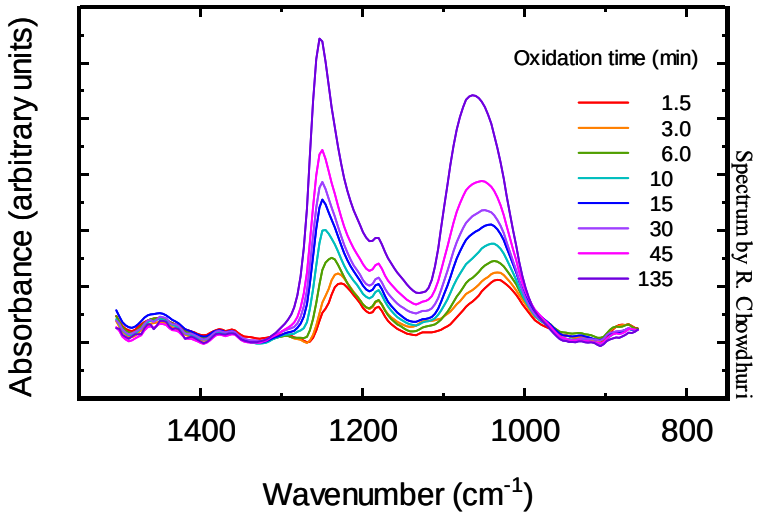


Figure 7: Major features in $SiO_2$ FT-IR LO Spectra. Note the LO peak at 1250 $cm^{-1}$ and the TO peak at 1050 $cm^{-1}$.

Figure 9: JEOL JEM2010F

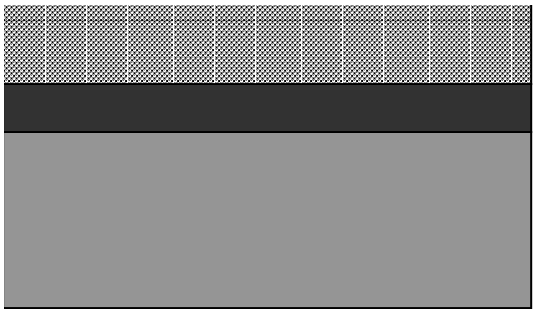

Figure 8: Annealing product

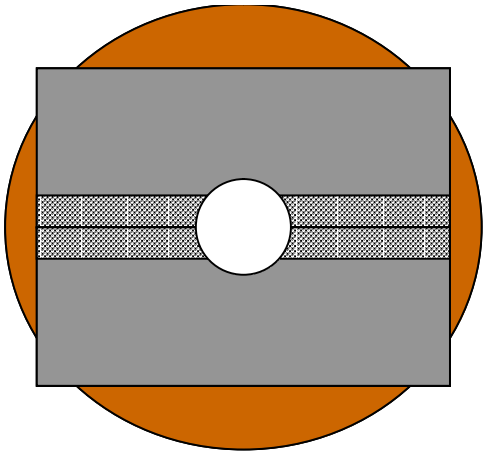

Figure 11a: Prepared STEM sample schematic

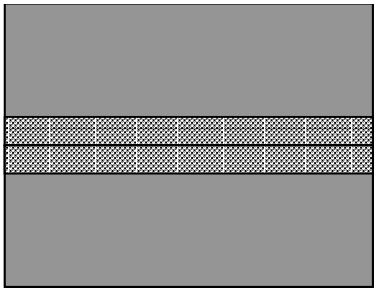

Figure 10: Cross sectional sample

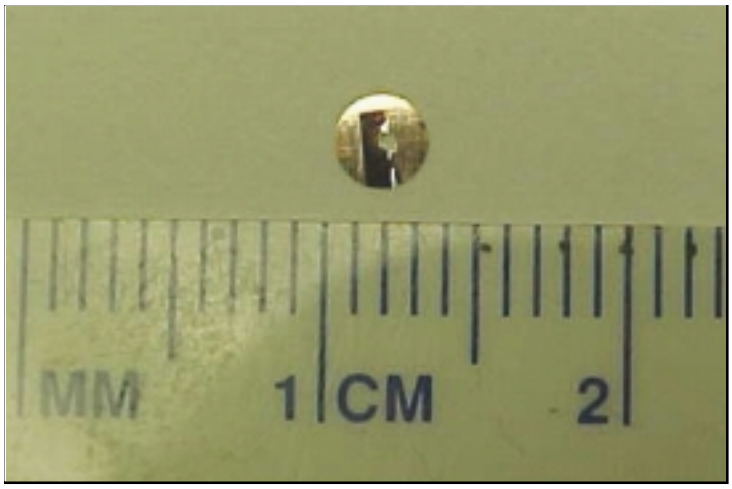


Figure 11b: Prepared STEM sample photograph

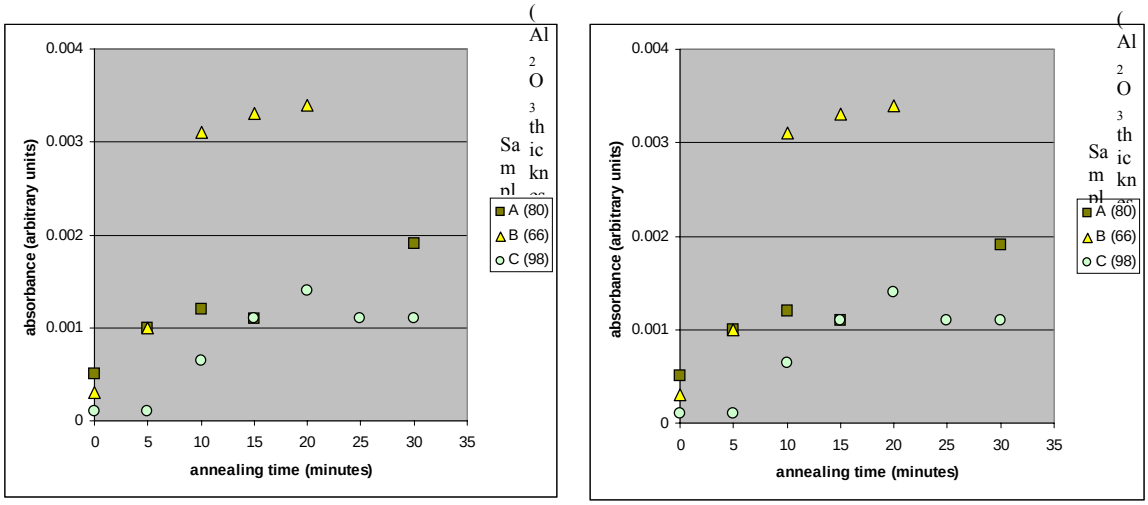


Annealing Temp.: 500°C

30 sccm samples

10 sccm samples

Figure 12: Peak intensity vs. annealing time

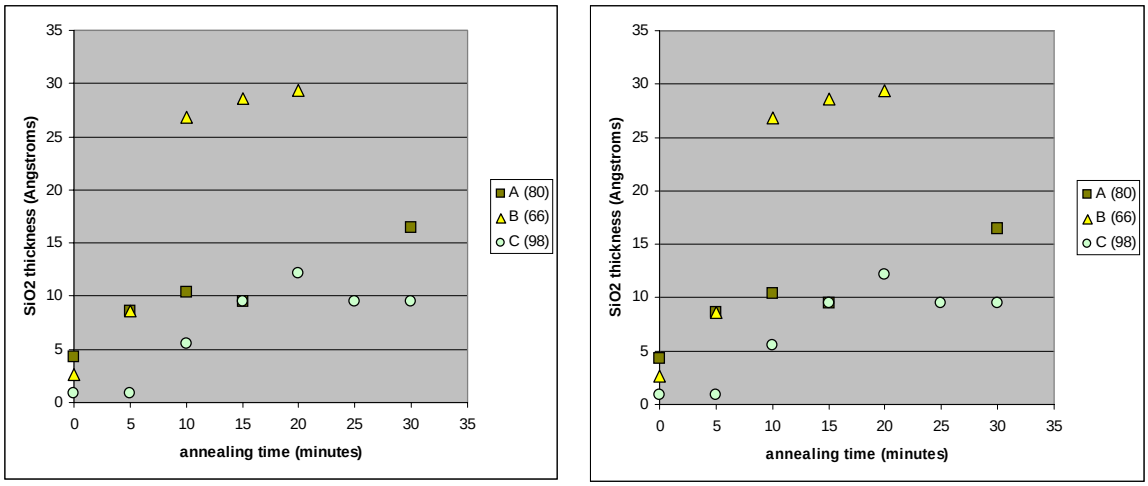


Annealing Temp.: 500°C

30 sccm samples 10 sccm samples

Figure 13: $SiO_2$ thickness vs. annealing time

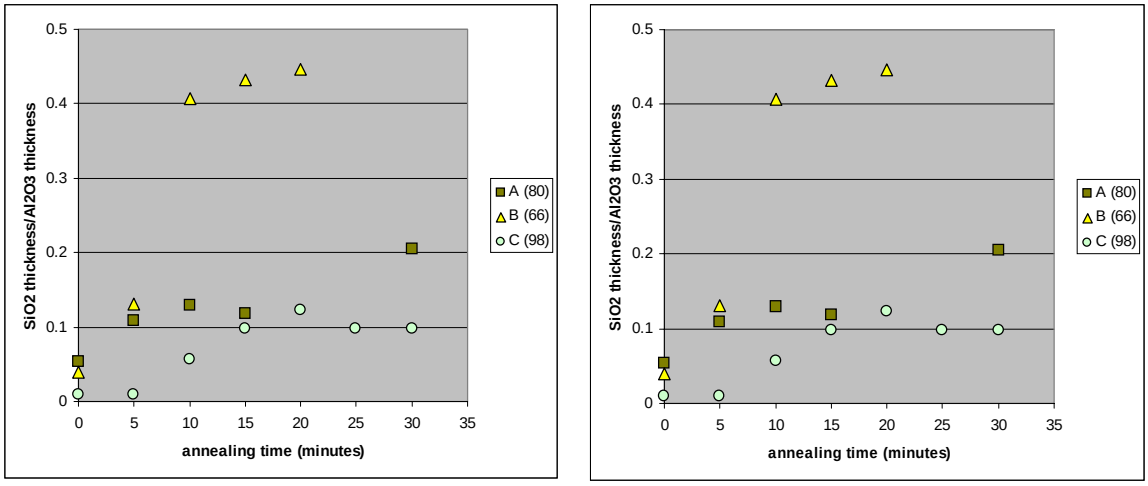


Annealing Temp.: 500°C

30 sccm samples 10 sccm samples

Figure 14: $SiO_2$ / $Al_2O_3$ thickness ratio vs. annealing time

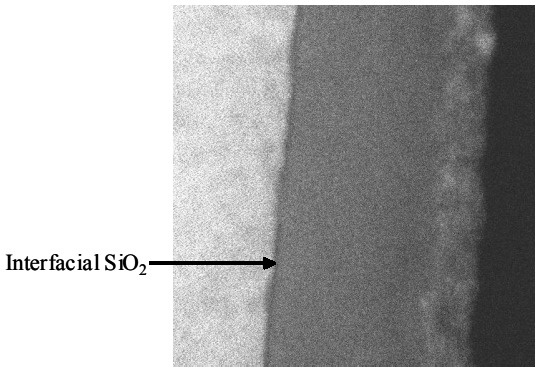


Figure 15

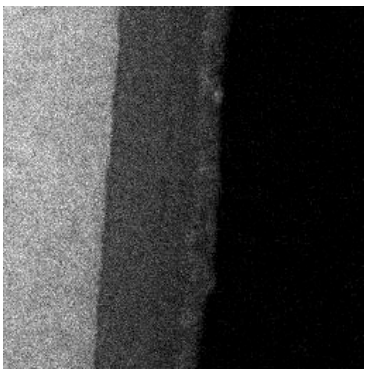

Figure 16

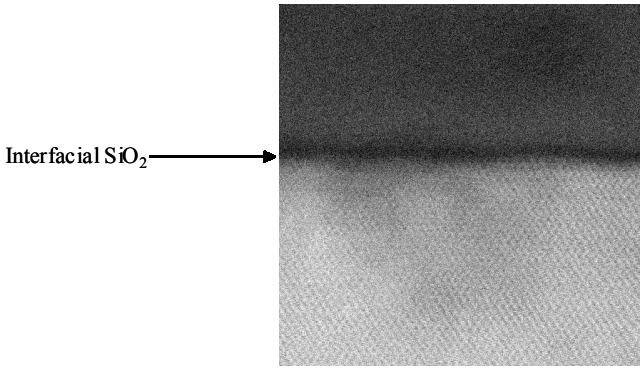


Figure 17

STEM Images form sample STEM020625-1